HHS Public Access

Author manuscript

Neuroimage. Author manuscript; available in PMC 2016 October 15.

Published in final edited form as:

Neuroimage. 2015 October 15; 120: 456–466. doi:10.1016/j.neuroimage.2015.07.007.

Monaural and binaural contributions to interaural-level-difference sensitivity in human auditory cortex

Christopher G. Stecker[a,*], **Susan A. McLaughlin**[b], and **Nathan C. Higgins**[a]

Susan A. McLaughlin: smcl@uw.edu; Nathan C. Higgins: nathan.higgins@vanderbilt.edu

[a]Department of Hearing and Speech Sciences, Vanderbilt University School of Medicine, Nashville, TN, USA

[b]Institute for Learning and Brain Sciences, University of Washington, Seattle, WA, USA

Abstract

Whole-brain functional magnetic resonance imaging was used to measure blood-oxygenation-level-dependent (BOLD) responses in human auditory cortex (AC) to sounds with intensity varying independently in the left and right ears. Echoplanar images were acquired at 3 Tesla with sparse image acquisition once per 12-second block of sound stimulation. Combinations of binaural intensity and stimulus presentation rate were varied between blocks, and selected to allow measurement of response-intensity functions in three configurations: monaural 55–85 dB SPL, binaural 55–85 dB SPL with intensity equal in both ears, and binaural with average binaural level of 70 dB SPL and interaural level differences (ILD) ranging ±30 dB (i.e., favoring the left or right ear). Comparison of response functions equated for contralateral intensity revealed that BOLD-response magnitudes (1) generally increased with contralateral intensity, consistent with positive drive of the BOLD response by the contralateral ear, (2) were larger for contralateral monaural stimulation than for binaural stimulation, consistent with negative effects (e.g., inhibition) of ipsilateral input, which were strongest in the left hemisphere, and (3) also increased with ipsilateral intensity when contralateral input was weak, consistent with additional, positive, effects of ipsilateral stimulation. Hemispheric asymmetries in the spatial extent and overall magnitude of BOLD responses were generally consistent with previous studies demonstrating greater bilaterality of responses in the right hemisphere and stricter contralaterality in the left hemisphere. Finally, comparison of responses to fast (40/s) and slow (5/s) stimulus presentation rates revealed significant rate-dependent adaptation of the BOLD response that varied across ILD values.

1. Introduction

The abilities of humans and other animals to accurately localize, segregate, and understand sound sources in space depends critically on binaural hearing. Auditory brainstem mechanisms compare inputs arriving from the two ears in order to assess differences in the

Corresponding author. g.christopher.stecker@vanderbilt.edu (C.G. Stecker).

Author contributions

GCS and SAM conceived and designed the experiment. GCS developed the experimental and analytical software. SAM and GCS conducted the experiment. GCS and SAM analyzed the data with help from NCH. GCS and SAM wrote the manuscript. GCS, SAM, and NCH edited the manuscript.

arrival time and intensity of sound at the ears, termed interaural time differences (ITD) and interaural level differences (ILD), respectively. Binaural processing throughout the auditory pathway involve both excitatory-excitatory interactions (e.g., temporal coincidence detection for ITD processing) and excitatory-inhibitory interactions that give rise to ILD sensitivity.

In mammals, the initial sites of binaural interaction are located within the brainstem superior olivary complex, but sensitivity to ITD and ILD is found throughout the auditory pathway. In the auditory cortex (AC), a majority of neurons exhibit binaural sensitivity (Kitzes, 2008), consistent with the observation that accurate sound localization in both humans and other mammals is profoundly disrupted by AC lesions (e.g., Jenkins and Masterton, 1982; Heffner, 1997; Zatorre and Penhune, 2001; Malhotra et al., 2004). The majority of binaurally sensitive neurons in AC respond best to contralateral stimulation, i.e. sounds presented to the contralateral ear, from within the contralateral hemifield, or with values of ITD or ILD favoring the contralateral ear. That contralateral bias is detectable at a neuronal population level (e.g., Nakamoto et al., 2004; Harrington et al., 2008) and also in human evoked potentials (Ungan et al., 2001; Palomäki et al., 2005; Salminen et al., 2009; Briley et al., 2013) and blood-oxygenation-level-dependent (BOLD) responses measured with functional magnetic resonance imaging (fMRI; Woldorff et al., 1999; Jäncke et al., 2002; Langers et al., 2007; Schönwiesner et al., 2007; Gutschalk and Steinmann, 2015). The current study aimed to parametrically quantify ILD sensitivity in the human AC in order to describe the shape of BOLD response-ILD functions in each hemisphere and better understand the nature of contralateral bias in human AC.

Several studies have reported contralateral biases in AC BOLD responses to monaural stimulation of the left and right ears (Jäncke et al., 2002; Langers et al., 2007; Woods et al., 2009). Those data are consistent with AC sensitivity to ILD (monaural stimulation being a special case of very large ILD), but do not systematically characterize ILD sensitivity *per se*. In particular, the specific contributions of binaural and monaural pathways to ILD sensitivity in AC BOLD responses have not been clearly delineated. In contrast to studies of ITD, in which contralateral preference (Krumbholz et al., 2005b; 2007; von Kriegstein et al., 2008; Johnson and Hautus, 2010) [though see Woldorff et al. (1999) and Ungan et al. (2001)] may be taken to indicate purely binaural sensitivity, apparent ILD tuning is likely to include some influence of monaural intensity cues, given the anatomical predominance of the crossed monaural pathway (see Stecker and Gallun, 2012). Moreover, to the extent that binaural interactions *do* play a role in ILD tuning of AC BOLD responses, it is not entirely clear whether such interactions predominantly facilitate or suppress the BOLD response. Of these possibilities, suppression is strongly implicated by studies reporting incomplete binaural summation (Jäncke et al., 2002; Krumbholz et al., 2005a; Woods et al., 2009). Even so, the specific nature of binaural interaction remains poorly understood in that attenuation of the binaural BOLD response might reflect some combination of ipsilaterally driven neural inhibition in the ascending pathway and/or occlusion of ipsilateral responses by a stronger contralateral response (Kimura, 2011). Although it is not possible to tease apart the various contributions of neuronal excitation and inhibition that contribute to the AC BOLD response, a major goal of this study was to better describe the positive and negative

influences of contralateral and ipsilateral input and infer, where possible, the types of binaural interactions that shape activity in human AC.

In this study, we measured response-ILD functions in the human AC using BOLD fMRI. Since the goal was to study ILD sensitivity parametrically, we presented sounds that varied in intensity at the two ears. In some conditions, sounds were presented monaurally to the left or right ear (i.e. monotically). In other conditions, sounds were presented with equal intensity at the two ears (diotically) across a range of average binaural level (ABL). In yet other conditions, sounds were presented with differing intensity at the two ears (dichotically). In that case, ABL was fixed and ILD varied across a range of values favoring the left or right ear. All of these conditions were intermixed within scanning runs, allowing for direct comparison of AC BOLD responses across binaurally distinct stimuli equated for differences in monaural intensity.

2. Methods

Data were collected in the Diagnostic Imaging Sciences Center at the University of Washington, Seattle. All procedures, including recruitment, consenting, and testing of human subjects followed the guidelines of the University of Washington Human Subjects Division and were reviewed and approved by the cognizant Institutional Review Board.

2.1. Subjects

Ten adults (four male) between 18–50 years of age participated in the study. All self-reported as right handed, with normal hearing and no history of neurological disorder. One participant was the second author, and another was a graduate student not directly involved in the project. Other participants were naive to the focus of the study and were paid for their participation. Standard procedures for informed consent were followed, and written consent obtained from all participants.

2.2. Stimuli and task

As illustrated in Fig. 1, stimuli comprised trains of Gabor clicks (Gaussian-windowed tone bursts) in which each click consisted of a 4 kHz cosine multiplied by a Gaussian temporal envelope with $\sigma = 221\mu s$. The resulting spectral bandwidth was also Gaussian, with $\sigma = 750$ Hz (half-maximal bandwidth ≈ 1.8 kHz). The peak-to-peak interclick interval (ICI) was either 3 ms for standard stimuli, or 2 ms for rare detection targets. Such stimuli carry psychophysically salient ITD and ILD cues, and have been used extensively to study listeners' sensitivity to those cues in numerous behavioral experiments (e.g., Stecker and Brown, 2010; Stecker et al., 2013). Depending on the stimulus condition, click trains consisted of either 32 clicks (train duration = 95 ms) or 4 clicks (train duration = 11 ms). Click trains were synthesized at 48.828 kHz (Tucker-Davis Technologies RP2.1, Alachua FL) and presented via piezoelectric insert earphones (Sensimetrics, Malden MA) enclosed within circumaural ear defenders. Combined, the ear defenders and foam inserts provide roughly 40 dB attenuation of outside noise.

Two stimulus parameters were manipulated: sound level and presentation rate. Levels ranged from 55 to 85 dB SPL and "silent" (−10 dB SPL[1]), and were assigned independently

in each ear to measure BOLD responses in selected binaural sound configurations indicated in Fig. 2. Configurations included an “ABL series” of diotic stimuli whose intensity was the same in both ears and varied from 55 to 85 dB SPL in 5 dB increments. These are indicated by the positive diagonal in Fig. 2; green text gives the values of average binaural level (ABL) in each case. Also included was an “ILD series” of dichotic stimuli with ILD ranging ±30 dB in 10 dB increments (by convention, negative values correspond to greater intensity in the left ear), a range that roughly encompasses the maximum values of ILD experienced at 4000 Hz by human listeners. These were presented at a constant ABL of 70 dB SPL. Stimuli included in the ILD series are indicated on the negative diagonal of Fig. 2, with red text indicating the ILD in each case. Also included, for comparison to the effects of changing intensity to each ear independently, were monotic stimuli applied to each ear at 55, 70, or 85 dB SPL (dark gray cells in Fig. 2), with the opposing ear held “silent” (−10 dB SPL). Finally, a “silent” configuration was included in which intensity at both ears was set to −10 dB SPL (black cell in Fig. 2).

Temporally sparse image acquisition (see Imaging, below; Hall et al., 1999) was employed to further reduce the effects of scanner noise. Image acquisition occurred at the end of each 12-s block of stimuli. Because BOLD responses are known to adapt or habituate following repeated presentation of similar or predictable stimuli (Harms and Melcher, 2002), one potential concern is that habituation of the response over the block duration could mask any stimulus dependence of BOLD responses that emerges early in the block but decays over time. Two approaches were taken to deal with such effects: First, the timing of auditory stimuli was randomized to reduce stimulus predictability. Second, stimuli were presented at one of two rates: a fast rate of 40 click trains per second and a slower rate of 5 click trains per second. Similar rates were shown by Harms and Melcher (2002) to produce very significant and very minor habituation effects, respectively. Comparing the magnitude of response across the two presentation rates allows an estimate of how much response habituation occurred, and whether such effects may have altered the apparent tuning to ILD.

Stimuli were presented in blocks of 12-s duration, with a single combination of binaural intensities and stimulation rate selected per block. During the block, 160 clicks were presented each second; these were arranged into 5 trains of 32 clicks each (“slow” condition) or 40 trains of 4 clicks each (“fast” condition). The total acoustic energy at either presentation rate was thus equal over each one-second epoch of the block. Click-train onset times were randomized within each second, with the constraint that inter-train gaps could not be shorter than 0 ms (i.e., trains could not overlap in time) or longer than 200 ms in the slow condition or 30 ms in the fast condition. Transition to the next block was triggered by EPI image acquisition each 12 seconds, at which time a new stimulus configuration was presented. Combinations of rate and intensity were presented in random order, with “silent” blocks occurring every 4th block. Three 11-minute runs were completed, each comprising 52 blocks, resulting in a total of 114 presentations of sound blocks (6 per rate/intensity combination) and 42 presentations of the silent condition over the course of the entire imaging session. Because AC BOLD responses are modulated by attention to sounds

[1]The apparatus was configured and triggered identically during sound and silent presentations; for “silent” stimulation, the sound level was simply reduced to −10 dB SPL, a value well below detection threshold in the scanning environment.

(Petkov et al., 2004) and by the direction of spatial attention (Rinne, 2010), we sought to ensure that subjects attended to the sounds, but not specifically to their spatial characteristics. Subjects were required to detect and to respond with a right forefinger button press to rare presentations (once per ~ 13 s) of deviant-pitch click trains resulting from shortened ICIs (2 ms).[2] Behavioral data collected while scanning confirmed that all listeners were engaged in the task (≥ 50 % hit rate within 2s of targets [mean 66%] and ≤ 25 % false-alarm rate [mean 6%], i.e. button press without target in previous 2s) during the imaging runs.

2.3. Imaging and analysis

MRI scanning was performed at 3 Tesla (Phillips Achieva, Eindhoven, The Netherlands). First, a high-resolution (1×1×1 mm^3) whole-head anatomical image was acquired using a T1-weighted magnetization-prepared rapid gradient echo (MPRAGE) sequence. A fieldmap image was then acquired, and later converted to magnitude and phase images for B0 unwarping of functional data. Whole-brain functional images were then acquired using sparse echoplanar imaging (EPI) once per 12 seconds, synchronized to the start of each stimulus presentation block (TR = 12 s, 32 transverse slices, 4.5 mm thickness, in-plane resolution 3×3 mm^2).

Each functional volume was resampled to 1×1×1 mm^3 isotropic resolution prior to motion correction, following the “anatomical space” approach outlined by Kang et al. (2007). That approach improves the effective spatial resolution of mapping functional data to the underlying anatomy across small head movements, and thus the accuracy with which functional data can be localized to the cortical surface. Subsequent preprocessing – comprising motion correction, B0 unwarping, and high-pass filtering (100s) – was implemented using FSL 4.1.2 (FMRIB, Oxford, UK). An initial 3-D functional analysis, contrasting all sound versus all silent blocks, was performed in FEAT to verify data quality and coregister functional volumes to anatomical images processed by Freesurfer 4.1 (Martinos Center for Biomedical Imaging, MGH, Boston). Cortical-surface data were then extracted from each functional volume without spatial smoothing and represented on the standard spherical surface for alignment across runs and subjects using Freesurfer. Using MATLAB (Mathworks, Natick MA), surface data were then projected to a flattened representation using an equal-area Mollweide projection (Woods et al., 2009) and resampled to a rectangular grid of 191×141 elements centered on the intersection of Heschl’s gyrus (HG) and Superior Temporal Gyrus (STG). Subsequent statistical analyses were computed on the BOLD timecourse in each grid element (hereafter termed “surface voxel”) following normalization to its overall mean (baseline) value per run. No smoothing of data, in 3-D space or on the cortical surface, was performed other than that which naturally follows from reconstruction across small head movements (Kang et al., 2007).

Voxelwise analyses are plotted for illustration in Fig. 3a. These compare BOLD responses across three stimulus conditions: stimulation of the left ear (green), right ear (red), or both ears (blue) at 70 dB SPL monaural intensity. Each surface voxel plots the cross-subject

[2]In order to present similarly detectable targets, the shortened ICI was applied to a single 32-click train in the slow condition, but to 8 consecutive 4-click trains in the fast condition.

mean response in units of percent signal change relative to silent blocks, thresholded at 0.5% signal change.

Stimulus-parametric analyses were based on a single AC region of interest (ROI) defined for each combination of subject and hemisphere, as follows: First, an overall mask (yellow outline in Fig. 3) was defined on the Freesurfer group-average surface (FSaverage) in each hemisphere, to liberally encompass the sound-driven regions of AC previously schematized by Woods et al. (2009) and Humphries et al. (2010). The mask extended mediolaterally to include the lateral surface of STG and the fundus of the sylvian fissure separating STG from the insular gyri, and rostrocaudally to contain the length of STG while avoiding regions of supramarginal gyrus and anterior temporal pole. For each hemisphere in each subject, the overall magnitude of sound-driven response was computed in each surface voxel falling within the AC mask by comparing the signal intensity for all sound blocks versus all silent blocks, and expressing the difference in units of percent signal change. Surface voxels with sound response ≥ 0.5 of the maximum value across voxels were included in the ROI for a given subject and hemisphere. Lower panels of Fig. 3 plot the degree of ROI overlap between subjects. In general, ROIs broadly sampled the masked region, with greatest overlap immediately anterior and posterior to HG.

The ROI definition employed here reflects the goals of the current study, which were to characterize the overall ILD sensitivity of BOLD response in AC, broadly defined as the region of sound-evoked response within the overall AC mask. By definition, voxels that did not exhibit sound-driven responses were omitted from the ROI; thus, the spatial extent of ROI varied across listeners, ranging from 2–16% of the masked surface area in the left hemisphere (mean 11%) and 2–15% in the right (mean 7%). Greater homogeneity of ROI sizes across listeners would have been preferred, but would have entailed the inclusion of more sound-insensitive voxels in some listeners than others. Instead, the analyses reported here characterize the intensity and ILD sensitivity derived from sound-driven AC BOLD responses in each listener, regardless of variation in spatial extent. A more detailed ROI-based analyses of the current data set was completed by McLaughlin (2013), who compared responses across 12 ROIs based on functional-field divisions proposed by Woods et al. (2009, 2010). Due to the larger number of ROI regions, listeners differed less in the spatial extent of sound-driven voxels within each ROI. The overall results were quite consistent with those reported here, but demonstrated greater ILD sensitivity in posterior than in anterior ROIs. Readers particularly interested in regional variation of these effects are thus encouraged to consult that reference.

Response data within AC ROIs were summarized for each subject by computing the mean normalized signal (percent of baseline units) across surface voxels for each stimulus combination. Group-average data were computed and plotted against ILD and ABL in two different ways: First, as the across-subject mean of percent signal change relative to baseline (e.g., Fig. 4a–b). Second, by normalizing the response-ILD or response-ABL function to the interval [0–1] for each subject and hemisphere prior to averaging across subjects (e.g., Fig. 4c–d). In both cases, standard error of the mean was calculated by bootstrapping the cross-subject mean response 1000 times (i.e., resampling subjects with replacement and computing the mean for each such sample; Efron and Tibshirani, 1986) and taking the

standard deviation of the resulting sampling distribution for each stimulus. Null-hypothesis significance testing was conducted similarly: after 1000-fold bootstrapping of the cross-subject mean responses in each condition, a statistic of interest (e.g., difference between conditions) was calculated for each of the 1000 bootstrap replicates, and the p-value computed directly. Thus, for difference tests, the proportion of bootstrapped differences falling at or below zero gives the (one-tailed) p-value that differences were not greater than zero. For such tests, no separate statistic (e.g. *t* or *F* value) exists; in lieu, the proportion is reported directly to one significant digit, e.g., p=.004, or if the proportion was zero, as $p <$. 001.

3. Results and discussion

3.1. Surface-based analysis of monaural and binaural responses

Fig. 3a illustrates the AC response to monaural stimulation of the left (green) and right ears (red), or diotic stimulation (blue), at 70 dB SPL monaural intensity, combining across fast and slow presentation rates. The primary purpose of these plots is to illustrate the general region of sound-driven responses in AC, the tuning of which was interrogated in detail using separate region-of-interest (ROI) analyses described below. Data are plotted on the flattened cortical surface (Woods et al., 2009) separately for the two hemispheres. The background image illustrates cortical surface curvature: dark gray for gyri (positive curvature) and lighter gray for sulci (negative curvature). A single contour at zero curvature is illustrated in white. Plots are centered on putative human AC, the region of intersection between Heschl's gyrus (HG) and superior temporal gyrus (STG). The yellow line outlines an overall AC mask for normalizing voxel counts and determining candidate surface voxels for inclusion in ROI analyses. Neighboring anatomical landmarks are labelled for reference. Overlaid on the anatomical data are plots of the across-subject mean BOLD response in each stimulus condition, in units of percent signal change relative to overall baseline. Clear sound-driven responses, exceeding 0.5% signal change relative to silent blocks, were observed surrounding HG and extending onto posterolateral STG in both hemispheres. The shape of activation pattern, which appears in Fig. 3 to surround HG rather than strongly include it, is consistent with current data on the tonotopic organization of human AC, given the high-frequency (4000 Hz) stimulus employed here. Specifically, several studies have demonstrated preference for low frequencies near the crest of HG, from which positive gradients of best frequency extend in both anterior and posterior directions (Formisano et al., 2003; Woods et al., 2009; Humphries et al., 2010; Da Costa et al., 2011; Thomas et al., 2015). Across those studies, the AC regions responding maximally to 4000 Hz have been reported to surround HG on the anterior, posterior, and occasionally medial sides.

It was initially expected that responses in both hemispheres would be greater in magnitude and more extensive following stimulation of the contralateral than the ipsilateral ear. Fig. 3a illustrates, instead, a clear hemispheric asymmetry in the extent of activation. In the left hemisphere, responses were indeed more widespread in response to contralateral (right-ear) stimulation than ipsilateral stimulation, as evidenced by the extensive red and magenta shading surrounding HG. Right-hemisphere responses, however, were less strongly contralateral, as indicated by extensive white shading throughout much of the activated

region. Arbitrarily adopting 0.5% signal change as an activation threshold, contralateral monaural stimulation activated a greater proportion of surface voxels in the left hemisphere (on average, 20% of the AC masked region in each subject, bootstrapped 95% confidence interval: [0.13–0.26]) than did ipsilateral monaural stimulation (5% of AC mask, c.i.: [.03–.07], $p < .001$). In the right hemisphere, contralateral and ipsilateral responses did not differ in extent (12% [.08–.19] vs 11% [.08–.15], $p = .37$). Binaural responses activated 16% [.10–.26] and 15% [.10–.24] of AC surface voxels in left and right hemispheres, respectively, and did not significantly differ from contralateral in either hemisphere ($p = .26$ in left, $p = .75$ in right).

3.2. Parametric response functions measured within subject-specific ROIs

To quantify response-ABL and response-ILD functions more directly, activation values were calculated within a region of interest (ROI) comprising sound-driven voxels within the AC cortical surface. An AC ROI was defined for each subject by high-resolution sampling of the cortical surface (Kang et al., 2007), projection of the data to two dimensions (Woods et al., 2009), and identification of AC surface "voxels" producing at least 50% of the maximum activation (across voxels) when contrasting all sound blocks with all silent blocks (see Methods). The spatial extent and intersubject overlap (not smoothed) of the resulting ROIs are plotted in Fig. 3b.

Fig. 4a plots group-mean response-ABL functions in each hemisphere's AC ROI, for diotic stimuli presented with ABL ranging 55–85 dB SPL (green text in Fig. 2). Consistent with how ROIs were defined, the overall sound-driven response was highly significant at 1.4% signal change in the left hemisphere and 1.9% in the right (both $p < .001$) when comparing signal change between silence and the lowest-intensity sound blocks (55 dB SPL). Modulation of the BOLD response by ABL provided an additional 1.4% signal change in the left hemisphere and 1.6% signal change in the right. The magnitude of response modulation was significant in both hemispheres ($p < .001$ in each). Neither response modulation by ABL, nor the overall sound-versus-silence comparison, differed between hemispheres ($p = .12$ and $p = .47$, respectively).

Mean response-ILD functions are plotted in Fig. 4b, for stimuli matched in ABL but ranging ± 30 dB ILD (red text in Fig. 2). Modulation of the BOLD signal by ILD was somewhat less than for ABL, ranging 1.1% signal change across ILD values in the left hemisphere, and 0.8% in the right. The smaller response range for ILD versus ABL presumably reflected the constant 70 dB ABL of all stimuli included in the ILD series. As was the case for ABL, however, the range of response modulation was significant in both hemispheres ($p < .001$) and did not differ between hemispheres ($p = .72$). Maximum responses were obtained for 30 dB contralateral ILD in both hemispheres; minimum responses were observed around 10–20 dB ipsilateral ILD.

Fig. 4c and d plot the mean response-ABL and response-ILD functions, respectively, computed after normalization to match the BOLD response range across subjects. That is, each subject's response-ABL or response-ILD function was scaled to exactly fit the range [0–1] prior to averaging across subjects. Fig. 4c reveals a very close correspondence between response-ABL functions obtained in the two hemispheres. For no value of ABL did the two hemispheres differ significantly in their normalized response. The response-ABL

slope from 60 to 80 dB SPL (i.e., excluding the extreme values) was .04 of the normalized response range per dB, regardless of hemisphere. Normalized response-ILD functions (Fig. 4d) were nearly mirror-symmetric across the two hemispheres, crossing over at 0 dB ILD and reaching a minimum at 10 dB ipsilateral ILD in each case. Across the range from 10 dB ipsilateral to 30 dB contralateral ILD, mean BOLD responses in both hemispheres grew linearly with a slope of .02 of response range per dB ILD.

3.3. Comparing binaural and monaural responses

A direct comparison of binaural and monaural response functions appears in Fig. 5. For each hemisphere, five response functions are plotted: Green diamonds replot the response-ABL functions from Fig. 4a as a function of contralateral-ear level (which, by definition, equals the ABL). Red open squares replot the response-ILD functions from Fig. 4b as a function of contralateral ear level. Note that the right-hemisphere plot appears flipped left-to-right relative to Fig. 4b, because in that hemisphere positive ILD values favor the ipsilateral (right) ear. The left-hemisphere plot, in contrast, is oriented identically to Fig. 4b. Black filled squares plot responses to 55, 70, and 85 dB monaural stimulation of the contralateral ear (white text in Fig. 2). Open (white) squares plot, on a separate axis, responses to monaural stimulation of the ipsilateral ear at 55, 70, and 85 dB SPL.

Whereas the response-ILD functions of Fig. 4b and d demonstrate clear positive effects of contralateral stimulation, direct comparison to monaural responses in Fig. 5 reveals that ILD tuning also reflects ipsilateral influences, which primarily inhibit or suppress the BOLD response. Especially in the left hemisphere, significantly larger BOLD responses were elicited by stimulation of the contralateral ear alone (black squares) than by diotic binaural stimulation at equivalent monaural intensities (green). Bootstrapped paired-differences test: p=.003, .001, .03 at 55, 70, and 85 dB SPL, respectively. A similar trend in right hemisphere was significant at 55 dB SPL (p=.01) but not at 70 or 85 dB SPL (p=.08, .6 respectively). That hemispheric difference is consistent with greater right-hemisphere response to ipsilateral sound as previously noted. Significant differences are highlighted by dotted ellipses in Fig. 5; at each intensity, the encircled values were significantly different from all points falling outside the ellipse, which otherwise did not differ from one another.

Several features of the response functions additionally demonstrate positive influences of the ipsilateral ear on the binaural BOLD response. Responses to ipsilateral monaural sound (white squares) were significantly greater than silence ($p < .001$) but significantly weaker than contralateral monaural responses (black squares, $p < .001$) at all intensities and in both hemispheres. Ipsilateral responses were significantly greater in the right than left hemisphere at 55–70 dB SPL ($p < .04$), although the opposite was true at 85 dB SPL (p=.006). Furthermore, the steeper slope of the response-ABL function (green) compared to the two contralateral response functions (black and gray), particularly in the right hemisphere, suggests that the growth in binaural intensity, as opposed to contralateral intensity alone, controls the growth of BOLD response. Ipsilateral positive drive is even more clearly evident in comparison of the red (ILD) and green (ABL) curves at low contralateral intensities of 55–60 dB SPL. Such stimuli elicited significantly greater responses when matched with intense ipsilateral sound (in the ILD series) than when ipsilateral and

contralateral intensities were equal (in the ABL series). That was true in both the left (p=.01 at 55 dB, p=.005 at 60 dB) and right (p=.004 at 55 dB, p=.009 at 60 dB) hemispheres. Had the ipsilateral influence on BOLD magnitude been purely suppressive, the opposite relationship should have been found. Above 60 dB contralateral ear level, the ABL and ILD curves did not significantly differ in either hemisphere, suggesting that in this range BOLD responses were dominated by contralateral responses and primarily inhibitory/suppressive binaural interactions.

3.4. Stimulus-rate-dependent adaptation of the BOLD response

In the sparse-imaging block paradigm, images are acquired at the end of each 12-second block of repeated auditory stimulation. Thus, images are mainly sensitive to sustained responses and insensitive to responses that adapt strongly to repeated stimulation. Although some aspects of the design – for example pseudo-random timing of stimulus presentation – were adopted to minimize such effects, response adaptation is known to affect AC responses. Harms and Melcher (2002) demonstrated AC BOLD adaptation to depend strongly on stimulus presentation rate; adaptation was minimal at slow rates (2–10 per second) and much stronger for fast rates (40/s). In this study, we presented sounds at two different rates: 5/s (“slow”) and 40/s (“fast”), while maintaining the overall energy and spectral content of the sounds. Each binaural intensity combination was studied at both slow and fast rates. Previous analyses (e.g. Figs. 3–5) combined data across rates. Here, we compare the two to estimate the degree of rate-dependent response adaptation in each case, and to determine whether adaptation effects interact with sensitivity to other features such as ILD.

Fig. 6a plots response-ILD functions (see Fig. 4b) separately for slow (filled symbols) and fast (open symbols) presentation rate. Consistent with Harms and Melcher (2002), the results demonstrate stronger responses to slow than to fast presentation rates, regardless of stimulus condition. The difference (slow minus fast), plotted in Fig. 6b, can be taken as a proxy measure of adaptation, and was significantly nonzero ($p < .01$) for all tested ILD values. Somewhat surprisingly, the degree of adaptation was not constant, but instead varied significantly, across ILD values. Asterisks (*) at top of Fig. 6b indicate significant pairwise differences in each hemisphere, obtained by bootstrap difference tests on all 21 pairs of ILD values in each hemisphere, controlling for false discovery rate (FDR) of 0.05 via the procedure of Benjamini and Hochberg (1995). In both hemispheres, the greatest adaptation effects were observed for 20 dB contralateral ILD. Left hemisphere responses exhibited an additional local maximum in the adaptation function for moderate ipsilateral ILD values. In general, this pattern of rate-dependent adaptation differs from that expected for pure response adaptation, because extreme ILD values produced the greatest overall responses but relatively weaker adaptation effects than intermediate values (see also Fig. 7a–b). Instead, the results suggest some degree of stimulus-specific adaptation which could relate to other aspects of the underlying neuronal tuning to ILD.

Fig. 6c–d plot response-ILD functions computed after per-subject normalization as in Fig. 4c–d. As in Fig. 4, the normalized response functions reveal more consistent response-function shapes across hemispheres. Three features seem particularly noteworthy: First, at

both rates, response-ILD functions show remarkable symmetry across the left and right hemispheres. In each case, the functions cross near 0 dB ILD, and show very similar normalized response magnitudes for contralateral ILDs. Second, as a consequence of greater adaptation for intermediate than midline ILD values, the “fast” functions appear shifted toward the midline relative to “slow” functions. Whereas responses to 0 dB ILD were near the minimum for slow presentations, that minimum shifted to 10 dB ipsilateral – an d responses to 0 dB ILD increased – for fast presentations. Third, responses at 20 dB contralateral ILD showed the largest effects of rate-dependent adaptation, consistent with the pattern of differences noted in Fig. 6b. Whereas for slow presentations, response-ILD functions in both hemispheres peaked at 20 dB contralateral ILD, response-ILD functions exhibited local minima at that value for fast presentations. That effect could arise in part due to saturation of the BOLD response to slow presentations of 30 dB contralateral ILD, or to weaker contributions by midline or ipsilateral populations at 30 dB ILD compared to more moderate values. Future studies that measure binaural tuning across a range of ABL (and, hence, putative saturation effects) could investigate the potential influence of BOLD saturation on these effects. Taken together, the results suggest that rate-dependent adaptation interacts with the population tuning that underlies BOLD sensitivity to ILD.

4. General discussion

4.1. Contralateral preference for ILD

The results reveal clear preferences for contralateral ILD in both hemispheres, demonstrating that the underlying neuronal responses are both (a) tuned to ILD and (b) biased so that the population response favors contralateral stimulation. The ILD tuning of individual units (neurons or subpopulations) cannot, of course, be determined from these data alone, but the current data appear generally consistent with neuronal population data (Harrington et al., 2008). The BOLD response tuning observed here would be consistent with broad contralateral tuning in individual units, as suggested by neurophysiological recordings in AC of other mammals (Stecker et al., 2005; Werner-Reiss and Groh, 2008; Yao et al., 2013), or equally consistent with a map-like collection of sharply-tuned units that more densely sample contralateral ILD values. The additional presence of ipsilateral positive drive of the BOLD response, especially in the right hemisphere, suggests that whatever the nature of representation in local units, both contralateral and ipsilateral responses must be present in each hemisphere (Imig and Adrián, 1977; Nakamoto et al., 2004; Stecker et al., 2005; Werner-Reiss and Groh, 2008; Briley et al., 2013).

Across ILD values, BOLD responses in both hemispheres were greatest for large contralateral ILD and declined monotonically with ILD to a minimum around 10 dB ipsilateral ILD. Midline (0 dB) ILD values evoked modest activity in both hemispheres, falling within the steeply sloping region of the response-ILD function rather than the region of maximal response. That observation is consistent with the need to maximize response *contrast*, rather than response *magnitude*, in the midline region (Harper and McAlpine, 2004), and coincides with single unit data for azimuth tuning in mammalian AC (Stecker et al., 2005; Werner-Reiss and Groh, 2008) as well as cortical adaptation data in humans (Salminen et al., 2009; Magezi and Krumbholz, 2010; Briley et al., 2013). The overlap

between hemispheric responses near 0 dB ILD also appears consistent with studies of sound localization following unilateral AC lesions in animal models. Substantial deficits reported in the contralesional field typically spare the frontal region, including up to 30° of the ipsilateral azimuthal hemifield (Jenkins and Masterton, 1982; Heffner, 1997; Harrington, 2002; Malhotra et al., 2004).

4.2. Relative excitatory and inhibitory influences of each ear on the AC BOLD response

ILD tuning in auditory neurons throughout the binaural pathway is shaped by the interactions of excitation and inhibition of activity by stimulation of the two ears. The current results demonstrate both types of influences on BOLD-response magnitude in human AC. Consistent with previous studies investigating the influence of acoustic intensity on BOLD responses (reviewed in Uppenkamp and Röhl, 2014), responses to monaural and diotic sounds increased with ABL. Similarly, responses to sounds with ILD favoring the contralateral ear grew monotonically with increasing contralateral ear level. Both results indicate facilitation of the AC BOLD response by contralateral sound. When ILD significantly favored the ipsilateral ear, we also noted response elevations consistent with positive effects (excitation or disinhibition) of responses to ipsilateral input (see Gutschalk and Steinmann, 2015). Thus, the results indicate enhancement of the BOLD response by both ears, in both hemispheres.

Evidence for suppression of the AC BOLD response by ipsilateral ear stimulation was also evident in the current results. Consistent with previous studies (Jäncke et al., 2002; Krumbholz et al., 2005a; Langers et al., 2007), larger responses were evoked by monaural contralateral stimulation than by equal-intensity binaural stimulation. That effect was most notable in the left hemisphere, consistent with weaker responses to ipsilateral sound than in the right, but was significant at low intensities in both hemispheres. Note particularly that binaural responses never exceeded contralateral monaural responses. Thus, the predominant impact of ipsilateral input on the AC BOLD response appears to be functionally suppressive or inhibitory.[3]

The reduction of BOLD responses by ipsilateral stimulation, which was especially clear at low intensities, raises a practical issue for fMRI studies of sound intensity. Fig. 5 reveals greater response modulation by ABL or ILD than by intensity of monaural stimulation of the contralateral ear, particularly in the right hemisphere. That is, the low end of the response dynamic range is shaped by suppressive rather than facilitative binaural interactions, and thus greater stimulus contrast should be obtained in experiments that present stimuli binaurally rather than monaurally.

4.3. The potential origins of BOLD modulation in neuronal excitation and inhibition

A comment should be made regarding the possible neuronal origins of positive and negative binaural influences on the AC BOLD response. These include binaural interactions in the auditory brainstem and ascending auditory pathway, potentially along with local neuronal

[3]In the nomenclature of classical binaural physiology, the overall AC BOLD response would appear to be classified “EE/I:” excited by monaural stimulation of either ear, and exhibiting primarily inhibitory binaural interactions (see Nakamoto et al., 2004).

inhibition arising within the cortex itself (Kyweriga et al., 2014). Based on the ubiquity of binaural excitatory-inhibitory interactions in the brainstem and the presence of clear ILD tuning in neurons of the superior olivary complex and inferior colliculus, we presume that the majority of BOLD modulation by ILD observed in the current data was "inherited" from the neuronal inputs to AC (Gutschalk and Steinmann, 2015). The BOLD increases and decreases we observe in AC presumably reflect combinations of neuronal excitation and inhibition in the ascending pathway, which cannot be easily teased apart but which combine to produce net positive and negative effects on responses in AC neurons, and consequently on BOLD responses.

With respect to local neuronal behavior, it is widely accepted that local excitatory and inhibitory activity may be difficult or impossible to distinguish on the basis of BOLD responses alone (e.g., Lauritzen et al., 2012). Thus, to the extent that local inhibition was present in the current study, its contribution is likely to have been underestimated. A reasonable possibility, in fact, is that some portion of the BOLD elevation by ipsilateral stimulation might actually reflect local *inhibition* at the neuronal level. Consideration of these factors suggests, for example, that increasing BOLD response with ipsilateral sound level might originate in (1) neuronal excitation at any level of the ascending pathway, (2) local neuronal inhibition within the imaged AC structures, or (3) reductions in sub-cortical inhibition of ipsilateral responses by contralateral sources. The latter possibility would imply an additional, negative, effect of the contralateral ear on AC BOLD magnitudes (see Section 4.5, below). Combinations of such influence, in fact, seem likely given the diversity of facilitatory, inhibitory, and mixed binaural interactions within populations of AC neurons (Nakamoto et al., 2004).

4.4. Hemispheric asymmetries: is the right hemisphere bilateral in a way that the left is not?

Several studies of binaural sensitivity in human AC have demonstrated hemispheric asymmetries in the cortical representation of auditory space. Several of those studies reveal that left hemisphere responses strongly favor contralateral stimuli, whereas right hemisphere responses appear more bilateral (Krumbholz et al., 2005b; Schönwiesner et al., 2007; Krumbholz et al., 2007; Magezi and Krumbholz, 2010; Briley et al., 2013). On that basis, Magezi and Krumbholz (2010) proposed a "three-channel" model of spatial representation in human AC, consisting of contralateral channels in both hemispheres and an additional ipsilateral channel exclusive to the right hemisphere. That hypothesis is also consistent with human lesion studies that demonstrate bilateral localization deficits following right-AC damage, but minimal localization deficits following left-AC damage (e.g., Griffiths et al., 1997; Zatorre and Penhune, 2001; Spierer et al., 2009). Puzzlingly, the opposite pattern (i.e., ipsilateral responses in left but not right AC) has been reported in several MEG-adaptation studies (Palomäki et al., 2005; Tiitinen et al., 2006; Salminen et al., 2010).

Briley et al. (2013) employed a continuous stimulation paradigm in which EEG responses were compared across shifts in sound location that varied in magnitude from 0 to 120 degrees azimuth. The results demonstrated parametric sensitivity to shift size across that range, and to the direction of shift (i.e. contralateral or ipsilateral) in left but not right AC.

Briley et al. modeled their results using a computational opponent-channel framework, which could account for hemispheric asymmetry in the EEG data through greater contralateral weighting in the left hemisphere and a more balanced representation of contralateral and ipsilateral inputs in the right hemisphere, even though the existence and tuning of the channels themselves was assumed to be symmetric across the hemispheres. That is, in contrast to the “three channel” model of Magezi and Krumbholz (2010), Briley et al. suggest that each AC hemisphere contains both contralateral and ipsilateral populations, the relative weighting of which is responsible for hemispheric asymmetries apparent in human neuroimaging data.

The current results are consistent in a number of respects with the hypotheses of Magezi and Krumbholz (2010) and Briley et al. (2013). First, larger responses to ipsilateral sound were noted in right than left hemisphere. That result was exhibited in both the spatial extent of cortical activation (Fig. 3) and in the magnitude of BOLD response (Fig. 5). Although both results support the same pattern of hemispheric asymmetry, the “extent” data suggest a nearly complete equivalence of contralateral and ipsilateral response in the right hemisphere, whereas the magnitude data suggest greater contralateral bias in that monaural contralateral responses were significantly larger than ipsilateral in both hemispheres at all intensities. It may be worth considering that the apparent degree – and perhaps direction – of hemispheric asymmetry could thus be affected by the relative sensitivity of various neuroimaging methods to widespread versus spatially restricted patterns of activity and their relation to cortical-surface anatomy. Second, evidence that ipsilateral stimulation reduces the BOLD response was very strong in the left hemisphere, and less consistent in the right hemisphere. That result is in accord with MEG data from Fujiki et al. (2002), who described suppression of ipsilateral but not contralateral responses in the left hemisphere, but symmetrical suppression of responses to both ears in the right hemisphere, during binaural listening. Other features of the current results appeared more similar across the hemispheres. For example, response-ILD functions in both hemispheres increased monotonically from 10 dB ipsilateral to 30 dB contralateral ILD. Such functions appeared roughly mirror symmetric across the hemispheres (e.g., always crossing at 0 dB), despite differences in function shape when response functions were computed for fast vs slow stimulus presentations, or when both were combined. In the context of the models proposed by Magezi and Krumbholz (2010) and Briley et al. (2013), that result suggests that graded responses to ILD in each hemisphere are dominated by the ILD tuning of contralateral units, which are distributed similarly in the two hemispheres.

4.5. Rate-dependent BOLD adaptation and the opponent-channel hypothesis

The models described in the previous section embody the “opponent-channel” framework for auditory space that has emerged from consideration of psychophysical (Boehnke and Phillips, 1999; Phillips, 2008), single-unit (Wise and Irvine, 1985; McAlpine et al., 2001; Stecker et al., 2005), and neuroimaging (Salminen et al., 2009; Magezi and Krumbholz, 2010; Briley et al., 2013) data. Such models posit that locations are represented by comparing the activity within two (or more) broadly tuned neuronal “channels,” for example a contralateral and an ipsilateral channel within each hemisphere. As noted earlier, the response-ILD functions measured in the current study are consistent with a contralaterally

biased opponent-channel model (Stecker et al., 2005), but do not rule out other possibilities such as local codes for ILD that oversample contralateral values (see Stecker and Middlebrooks, 2003).

The opponent-channel hypothesis provides a possible account for another puzzling aspect of the current results, namely the variation in rate-dependent adaptation with ILD (Fig. 6b). If rate-dependent adaptation reflects habituation of sustained activity ("response adaptation"), then larger adaptation effects should be observed for stimuli that strongly excite large populations of neurons. Consistent with that expectation and the opponent-channel hypothesis of Stecker et al. (2005), greater adaptation was observed for intermediate ILD values that should strongly excite one or the other population. Less adaptation was observed for midline values that simultaneously but more weakly excite both populations. Less consistent with this account are the data for extreme ILD values, which ought to strongly activate the contralateral channel but do not evoke maximal response adaptation. A simple descriptive model of those effects is illustrated in Fig. 7a–b, which plots responses of both contralateral (violet) and ipsilateral (green) populations within a single hemisphere. In the model, response adaptation in each population is proportional to the magnitude of that population's response; thus, given contralateral bias in the overall (summed) response, greater adaptation is predicted for contralateral than ipsilateral ILD values (solid line in Fig. 7b).

An alternative to the "response adaptation" account of the data in Fig. 6 is that rate-dependent adaptation reflects inhibition or "forward suppression" in the ascending pathway, which grows in effectiveness with repeated stimulation (i.e., over the course of each block). Single-unit data in cat AC suggest that enhanced selectivity emerges in this manner and helps to segregate the neuronal population responses to competing objects in the auditory scene (Middlebrooks and Bremen, 2013). The idea offers an appealing account of the adaptation profile of Fig. 6b, which is illustrated via descriptive modeling in Fig. 7c–d. In the model, response reduction via forward suppression is proportional to the ratio of activity in the contralateral and ipsilateral populations, with the contralateral population suppressing the ipsilateral response and vice versa. Thus, stimuli with 0 dB ILD activate both populations in a relatively balanced manner, and neither strongly inhibits the other. Intermediate ILD values shift the balance to favor one of the populations; its ability to inhibit the other population increases as a result. The time course of that effect is not illustrated in the model, but suppression is expected to grow with repeated stimulation, especially for high-rate stimulation, resulting in large apparent adaptation effects at the end of each block. More extreme ILD values result in highly imbalanced cortical activation, such that strong (perhaps complete) inhibition of the weakly driven population emerges rapidly and does not change much over the block. Thus, the overall magnitude of forward suppression appears tuned to ILD in each population; summing across populations (solid line in Fig. 7d) reveals a multi-peaked adaptation function comparable to the fMRI data. Future work should attempt to address this possibility at a single-unit level to determine how neuronal subpopulations with different tuning to ILD adapt to repeated high-rate stimulation.

Finally, we note that the adaptation data in Fig. 6b do not follow the hemispheric asymmetry for monotic sounds described in the previous section. Here, the right hemisphere demonstrates significantly stronger adaptation effects for contralateral 20 dB than ipsilateral 10 dB ILD (the local maxima, p=.04) whereas the same values in left hemisphere produce nearly equal adaptation (p=.4). That is, in terms of adaptation the left hemisphere appears bilateral, and the right contralateral – a pattern opposite to the hemispheric asymmetry in responses to monotic sounds but consistent with that reported by Salminen et al. (2010).

Acknowledgments

The authors thank Jenee O'Brien, Jeff Stevenson, and Ken Maravilla for assistance with fMRI data collection; Clark Johnson for help with data processing, particularly with respect to B0 unwarping; Andrew Brown, Ione Fine, Geoff Boynton, Fang Jiang, and Len Kitzes for helpful comments during the design phase; and Andrew Brown, Teemu Rinne, and two anonymous reviewers, for comments on earlier versions of this manuscript. This study was supported by the National Science Foundation (NSF; DBI-0107567) and National Institute On Deafness And Other Communication Disorders (NIDCD; R03 DC009482-02S1, R01 DC011548, and T32 DC005361). The content is solely the responsibility of the authors and does not necessarily represent the official views of the NSF, NIDCD, or the National Institutes of Health. Portions of this work, including alternate analyses, appeared in the second author's Ph.D. dissertation (McLaughlin, 2013).

References

Benjamini Y, Hochberg Y. Controlling the false discovery rate: a practical and powerful approach to multiple testing. J R Stat Soc Ser B. 1995; 57(1):289–300.

Boehnke SE, Phillips DP. Azimuthal tuning of human perceptual channels for sound location. J Acoust Soc Am. 1999 Oct; 106(4 Pt 1):1948–1955. [PubMed: 10530019]

Briley PM, Kitterick PT, Summerfield AQ. Evidence for opponent process analysis of sound source location in humans. J Assoc Res Otolaryngol. 2013; 14:83–101. [PubMed: 23090057]

Da Costa S, van der Zwaag W, Marques JP, Frackowiak RSJ, Clarke S, Saenz M. Human primary auditory cortex follows the shape of heschl's gyrus. J Neurosci. 2011 Oct; 31(40):14067–14075. [PubMed: 21976491]

Efron B, Tibshirani R. Bootstrap methods for standard errors, confidence intervals, and other measures of statistical accuracy. Stat Sci. 1986; 1(1):54–75.

Formisano E, Kim DS, Di Salle F, van de Moortele PF, Ugurbil K, Goebel R. Mirror-symmetric tonotopic maps in human primary auditory cortex. Neuron. 2003 Nov; 40(4):859–869. [PubMed: 14622588]

Fujiki N, Jousmäki V, Hari R. Neuromagnetic responses to frequency-tagged sounds: A new method to follow inputs from each ear to the human auditory cortex during binaural hearing. J Neurosci. 2002; 22(RC205):1–4. [PubMed: 11756482]

Griffiths TD, Rees A, Witton C, Cross PM, Shakir RA, Green GG. Spatial and temporal auditory processing deficits following right hemisphere infarction. a psychophysical study. Brain. 1997 May; 120(Pt 5):785–794. [PubMed: 9183249]

Gutschalk A, Steinmann I. Stimulus dependence of contralateral dominance in human auditory cortex. Hum Brain Mapp. 2015 Oct; 36(3):883–896. [PubMed: 25346487]

Hall DA, Haggard MP, Akeroyd MA, Palmer AR, Summerfield AQ, Elliott MR, Gurney EM, Bowtell RW. "Sparse" temporal sampling in auditory fMRI. Hum Brain Mapp. 1999; 7(3):213–223. [PubMed: 10194620]

Harms MP, Melcher JR. Sound repetition rate in the human auditory pathway: representations in the waveshape and amplitude of fMRI activation. J Neurophysiol. 2002 Sep; 88(3):1433–1450. [PubMed: 12205164]

Harper NS, McAlpine D. Optimal neural population coding of an auditory spatial cue. Nature. 2004 Aug; 430(7000):682–686. [PubMed: 15295602]

Harrington, IA. PhD thesis. The University of Toledo; 2002. Effect of auditory cortex lesions on discriminations of frequency changes, amplitude change and sound location by Japanese macaqes (*Macaca fuscata*).

Harrington IA, Stecker GC, Macpherson EA, Middlebrooks JC. Spatial sensitivity of neurons in the anterior, posterior, and primary fields of cat auditory cortex. Hear Res. 2008 Jun; 240(1–2):22–41. [PubMed: 18359176]

Heffner HE. The role of macaque auditory cortex in sound localization. Acta Otolaryngol Suppl. 1997; 532:22–27. [PubMed: 9442840]

Humphries C, Liebenthal E, Binder JR. Tonotopic organization of human auditory cortex. NeuroImage. 2010 Apr; 50(3):1202–1211. [PubMed: 20096790]

Imig TJ, Adrián HO. Binaural columns in the primary field (a1) of cat auditory cortex. Brain Res. 1977 Dec; 138(2):241–257. [PubMed: 589474]

Jäncke L, Wüstenberg T, Schulze K, Heinze HJ. Asymmetric hemodynamic responses of the human auditory cortex to monaural and binaural stimulation. Hear Res. 2002 Aug; 170(1–2):166–178. [PubMed: 12208550]

Jenkins WM, Masterton RB. Sound localization: effects of unilateral lesions in central auditory system. J Neurophysiol. 1982 Jun; 47(6):987–1016. [PubMed: 7108581]

Johnson BW, Hautus MJ. Processing of binaural spatial information in human auditory cortex: neuromagnetic responses to interaural timing and level differences. Neuropsychologia. 2010; 48:2610–2619. [PubMed: 20466010]

Kang X, Yund EW, Herron TJ, Woods DL. Improving the resolution of functional brain imaging: analyzing functional data in anatomical space. Magn Reson Imaging. 2007 Sep; 25(7):1070–1078. [PubMed: 17707169]

Kimura D. From ear to brain. Brain Cogn. 2011; 76:214–217. [PubMed: 21236541]

Kitzes L. Binaural interactions shape binaural response structures and frequency response functions in primary auditory cortex. Hear Res. 2008 Apr; 238(1–2):68–76. [PubMed: 18295994]

Krumbholz K, Schönwiesner M, Rübsamen R, Zilles K, Fink GR, von Cramon DY. Hierarchical processing of sound location and motion in the human brainstem and planum temporale. Eur J Neurosci. 2005a Jan; 21(1):230–238. [PubMed: 15654860]

Krumbholz K, Schönwiesner M, von Cramon DY, Rübsamen R, Shah NJ, Zilles K, Fink GR. Representation of interaural temporal information from left and right auditory space in the human planum temporale and inferior parietal lobe. Cereb Cortex. 2005b Mar; 15(3):317–324. [PubMed: 15297367]

Krumbholz K, Hewson-Stoate N, Schönwiesner M. Cortical response to auditory motion suggests an asymmetry in the reliance on inter-hemispheric connections between the left and right auditory cortices. J Neurophysiol. 2007 Feb; 97(2):1649–1655. [PubMed: 17108095]

Kyweriga M, Stewart W, Cahill C, Wehr M. Synaptic mechanisms underlying interaural level difference selectivity in rat auditory cortex. J Neurophysiol. 2014; 112:2561–2571. [PubMed: 25185807]

Langers DRM, Backes WH, van Dijk P. Representation of lateralization and tonotopy in primary versus secondary human auditory cortex. NeuroImage. 2007 Jan; 34(1):264–273. [PubMed: 17049275]

Lauritzen M, Mathiesen C, Schaefer K, Thomsen KJ. Neuronal inhibition and excitation, and the dichotomic control of brain hemodynamic and oxygen responses. NeuroImage. 2012 Aug; 62(2): 1040–1050. [PubMed: 22261372]

Magezi DA, Krumbholz K. Evidence for opponent-channel coding of interaural time differences in human auditory cortex. J Neurophysiol. 2010 Oct; 104(4):1997–2007. [PubMed: 20702739]

Malhotra S, Hall AJ, Lomber SG. Cortical control of sound localization in the cat: unilateral cooling deactivation of 19 cerebral areas. J Neurophysiol. 2004 Sep; 92(3):1625–1643. [PubMed: 15331649]

McAlpine D, Jiang D, Palmer AR. A neural code for low-frequency sound localization in mammals. Nat Neurosci. 2001 Apr; 4(4):396–401. [PubMed: 11276230]

McLaughlin, SA. PhD thesis. University of Washington; 2013. Functional magnetic resonance imaging of human auditory cortical tuning to interaural level and time differences.

Middlebrooks JC, Bremen P. Spatial stream segregation by auditory cortical neurons. J Neurosci. 2013 Jul; 33(27):10986–11001. [PubMed: 23825404]

Nakamoto KT, Zhang J, Kitzes LM. Response patterns along an isofrequency contour in cat primary auditory cortex (ai) to stimuli varying in average and interaural levels. J Neurophysiol. 2004 Jan; 91(1):118–135. [PubMed: 14523080]

Palomäki KJ, Tiitinen H, Mäkinen V, May PJC, Alku P. Spatial processing in human auditory cortex: the effects of 3d, itd, and ild stimulation techniques. Brain Res Cogn Brain Res. 2005 Aug; 24(3): 364–379. [PubMed: 16099350]

Petkov CI, Kang X, Alho K, Bertrand O, Yund EW, Woods DL. Attentional modulation of human auditory cortex. Nat Neurosci. 2004 Jun; 7(6):658–663. [PubMed: 15156150]

Phillips DP. A perceptual architecture for sound lateralization in man. Hear Res. 2008 Apr; 238(1–2): 124–132. [PubMed: 17980984]

Rinne T. Activations of human auditory cortex during visual and auditory selective attention tasks with varying difficulty. Open Neuroimaging J. 2010; 4:187–193.

Salminen NH, May PJC, Alku P, Tiitinen H. A population rate code of auditory space in the human cortex. PLoS One. 2009; 4(10):e7600. [PubMed: 19855836]

Salminen NH, Tiitinen H, Miettinen I, Alku P, May PJC. Asymmetrical representation of auditory space in human cortex. Brain Res. 2010 Jan.1306:93–99. [PubMed: 19799877]

Schönwiesner M, Krumbholz K, Rübsamen R, Fink GR, von Cramon DY. Hemispheric asymmetry for auditory processing in the human auditory brain stem, thalamus, and cortex. Cereb Cortex. 2007 Feb; 17(2):492–499. [PubMed: 16565292]

Spierer L, Bellmann-Thiran A, Maeder P, Murray MM, Clarke S. Hemispheric competence for auditory spatial representation. Brain. 2009 Jul; 132(Pt 7):1953–1966. [PubMed: 19477962]

Stecker GC, Brown AD. Temporal weighting of binaural cues revealed by detection of dynamic interaural differences in high-rate gabor click trains. J Acoust Soc Am. 2010; 127(5):3092–3103. [PubMed: 21117758]

Stecker, GC.; Gallun, FJ. Binaural hearing, sound localization, and spatial hearing. In: Tremblay, K.; Burkard, R., editors. Translational perspectives in auditory neuroscience: Normal aspects of hearing. Vol. Ch 14. Plural Publishing; San Diego: 2012. p. 387-437.

Stecker GC, Middlebrooks JC. Distributed coding of sound locations in the auditory cortex. Biol Cybern. 2003; 89(5):341–349. [PubMed: 14669014]

Stecker GC, Harrington IA, Middlebrooks JC. Location coding by opponent neural populations in the auditory cortex. PLoS Biol. 2005; 3(3):e78. [PubMed: 15736980]

Stecker GC, Ostreicher JD, Brown AD. Temporal weighting functions for interaural time and level differences. III Temporal weighting for lateral position judgments. J Acoust Soc Am. 2013 Aug; 134(2):1242–1252. [PubMed: 23927122]

Thomas JM, Huber E, Stecker GC, Boynton GM, Saenz M, Fine I. Population receptive field estimates of human auditory cortex. NeuroImage. 2015 Jan.105:428–439. [PubMed: 25449742]

Tiitinen H, Salminen NH, Palomäki KJ, Mäkinen VT, Alku P, May PJC. Neuromagnetic recordings reveal the temporal dynamics of auditory spatial processing in the human cortex. Neurosci Lett. 2006 Mar; 396(1):17–22. [PubMed: 16343772]

Ungan P, Yagcioglu S, Goksoy C. Differences between the n1 waves of the responses to interaural time and intensity disparities: scalp topography and dipole sources. Clin Neurophysiol. 2001 Mar; 112(3):485–498. [PubMed: 11222971]

Uppenkamp S, Röhl M. Human auditory neuroimaging of intensity and loudness. Hear Res. 2014 Jan. 307:65–73. [PubMed: 23973563]

von Kriegstein K, Griffiths TD, Thompson SK, McAlpine D. Responses to interaural time delay in human cortex. J Neurophysiol. 2008 Nov; 100(5):2712–2718. [PubMed: 18799604]

Werner-Reiss U, Groh JM. A rate code for sound azimuth in monkey auditory cortex: implications for human neuroimaging studies. J Neurosci. 2008 Apr; 28(14):3747–3758. [PubMed: 18385333]

Wise LZ, Irvine DR. Topographic organization of interaural intensity difference sensitivity in deep layers of cat superior colliculus: implications for auditory spatial representation. J Neurophysiol. 1985 Aug; 54(2):185–211. [PubMed: 4031984]

Woldorff MG, Tempelmann C, Fell J, Tegeler C, Gaschler-Markefski B, Hinrichs H, Heinz HJ, Scheich H. Lateralized auditory spatial perception and the contralaterality of cortical processing as studied with functional magnetic resonance imaging and magnetoencephalography. Hum Brain Mapp. 1999; 7(1):49–66. [PubMed: 9882090]

Woods DL, Stecker GC, Rinne T, Herron TJ, Cate AD, Yund EW, Liao I, Kang X. Functional maps of human auditory cortex: effects of acoustic features and attention. PLoS One. 2009; 4(4):e5183. [PubMed: 19365552]

Woods DL, Herron TJ, Cate AD, Yund EW, Stecker GC, Rinne T, Kang X. Functional properties of human auditory cortical fields. Front Syst Neurosci. 2010; 4:155. [PubMed: 21160558]

Yao JD, Bremen P, Middlebrooks JC. Rat primary auditory cortex is tuned exclusively to the contralateral hemifield. J Neurophysiol. 2013 Nov; 110(9):2140–2151. [PubMed: 23945782]

Zatorre RJ, Penhune VB. Spatial localization after excision of human auditory cortex. J Neurosci. 2001 Aug; 21(16):6321–6328. [PubMed: 11487655]

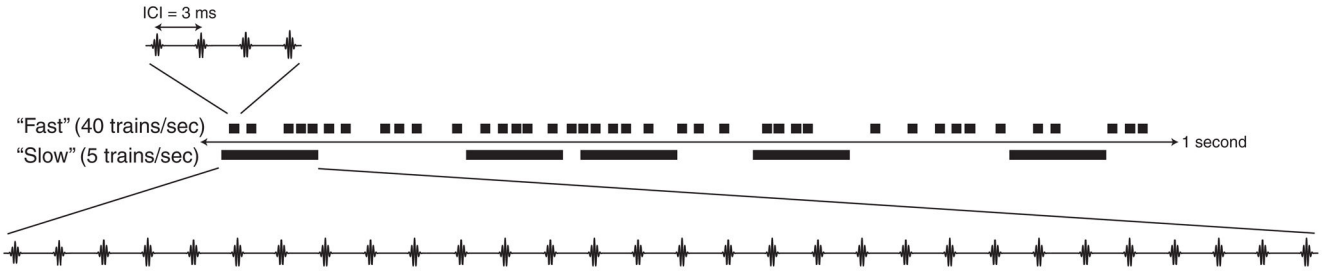

Fig. 1.

Stimuli employed in the study were narrowband filtered impulses (Gabor clicks) with 4000 Hz center frequency. Clicks were presented in trains with 3 ms interclick interval (ICI). Sounds were presented throughout each imaging block, but with timing randomized in an effort to enhance cortical responsiveness. Two conditions were tested for each combination of binaural intensities. In the "slow" condition, each second of sound presented 5 trains of 32 clicks each, whereas in the "fast" condition each second of sound presented 40 trains of 4 clicks each. The total number of clicks presented was 160 per second regardless of condition. Thus, overall intensity and spectral bandwidth were identical, while the degree of periodicity (i.e. noisiness) and number of onset events differed. The presentation time of each click train was randomized within each one-second epoch of stimulation, with constraints to avoid overlap or excessive clustering of successive trains. Images were acquired following 12 such one-second epochs, each with independently randomized stimulus timing.

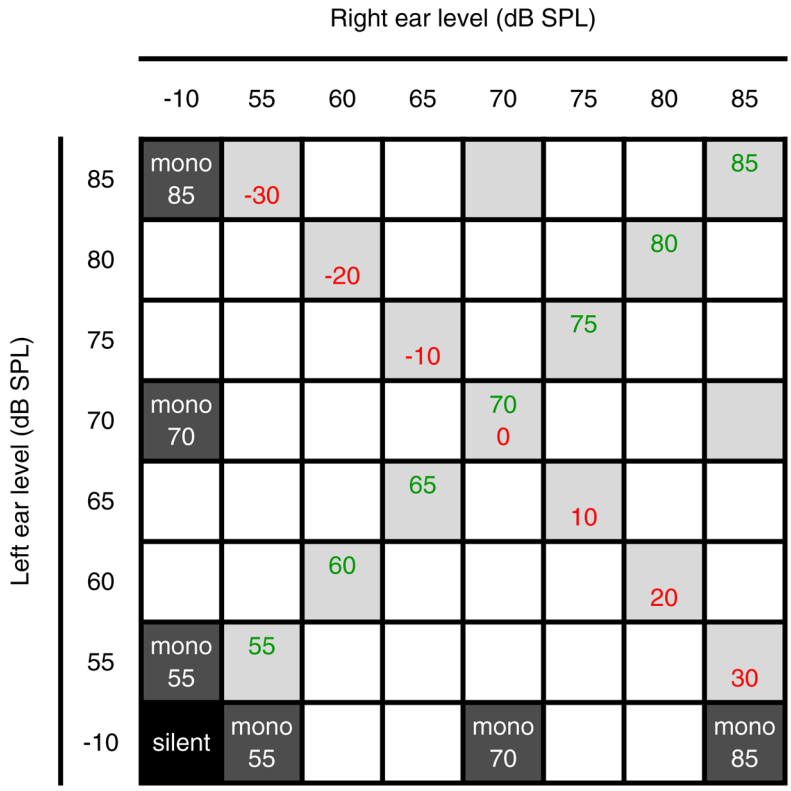

Fig. 2.

Binaural intensity combinations of click train stimuli are indicated in a matrix, with left-ear intensity level indicated on the vertical and right-ear level on the horizontal. Shaded cells indicate binaural level combinations presented in the experiment. These included: 1) a "silent" combination (both ears set to −10 dB SPL, indicated by the black cell in lower left corner), 2) monaural presentation at 55, 70, and 85 dB SPL at each ear (dark gray cells in left column and bottom row; opposite ear is silent) and 3) the corresponding combinations in which the opposite ear was fixed at 85 dB SPL (e.g., shaded but unlabeled cells), 4) binaural presentation with varying but equal intensity at the two ears (positive diagonal; green text indicates the average binaural level [ABL]), and 5) binaural presentation with intensity varying oppositely in the two ears (negative diagonal; red text gives the interaural level difference [ILD] in each case).

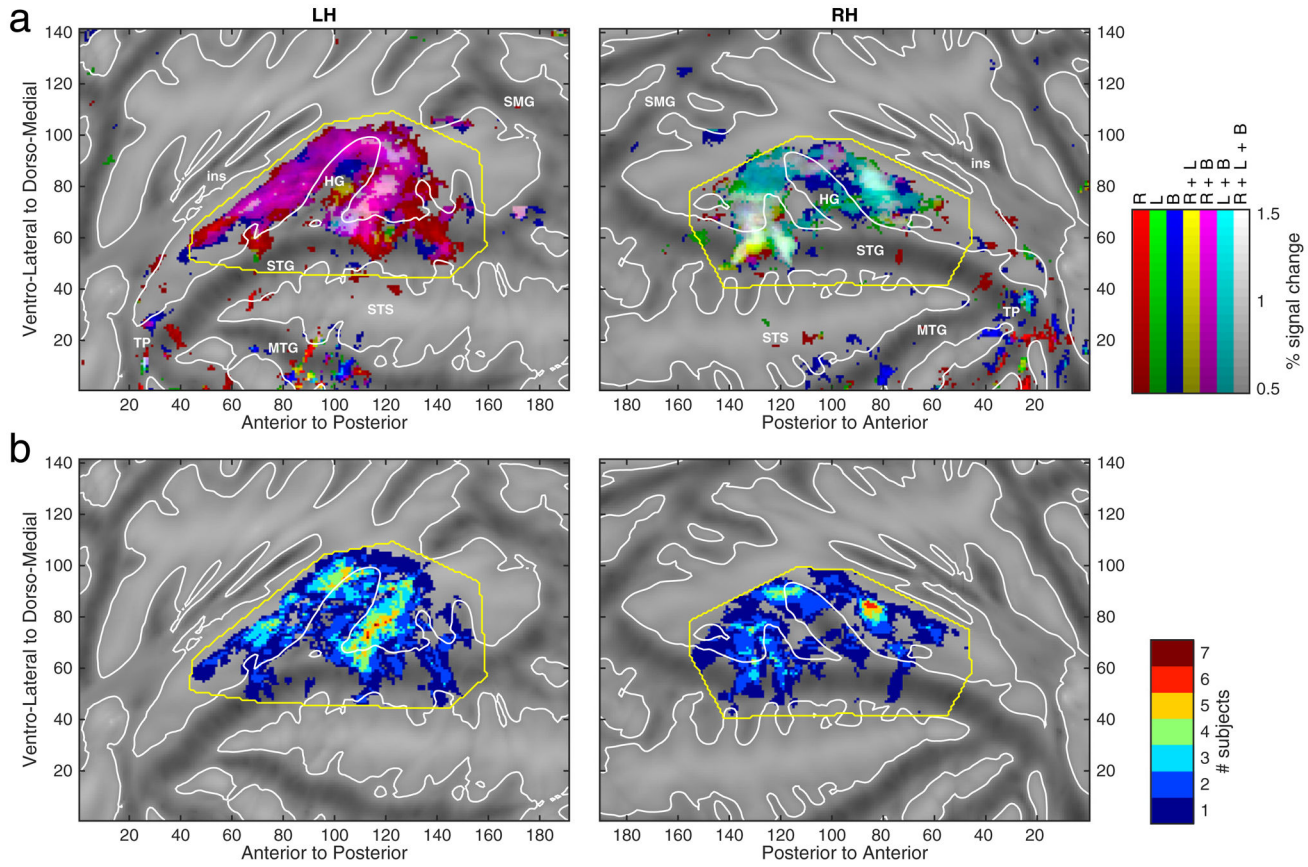

Fig. 3.

Surface plots illustrating the extent and magnitude of sound-driven responses in auditory cortex. (a): Group-mean BOLD response magnitude is plotted in units of percent signal change relative to overall baseline, in left (LH) and right (RH) AC. In each panel, response data for three conditions are overlaid: responses to 70 dB monaural stimulation of the right ear (R) appear in red, 70 dB monaural stimulation of the left ear (L) in green, and 70 dB binaural stimulation (B) in blue. Color maps (scale at right) overlap, so that magenta indicates equal response to right (red) and binaural (blue) stimulation, etc. Images are thresholded at 0.5% signal change, but not otherwise masked. Responses were primarily localized to the region surrounding Heschl's gyrus (HG) and posterolateral superior temporal gyrus (STG). Other anatomical landmarks are indicated for orientation: superior temporal sulcus (STS), middle temporal gyrus (MTG), the anterior temporal pole (TP), supramarginal gyrus (SMG), and gyri of the insula (ins). Left-hemisphere responses were strongly dominated by the contralateral right ear (red [R] and magenta [R + B] shading), whereas right-hemisphere responses were more sensitive to binaural and ipsilateral stimulation (note extensive regions of white [R + L + B] shading). (b): Regions included within AC ROIs for parametric analysis. An ROI for each hemisphere in each subject was defined to contain sound-responsive surface voxels, by including only those voxels with sound (vs. silence) responses at least 50% of the maximum sound response across voxels. Color indicates the number of subjects for whom the corresponding voxel was included in the analytical ROI, i.e. the degree of ROI overlap between subjects. Note that no smoothing

was applied to the data. Yellow line indicates the initial mask used to identify candidate voxels for inclusion in the ROI.

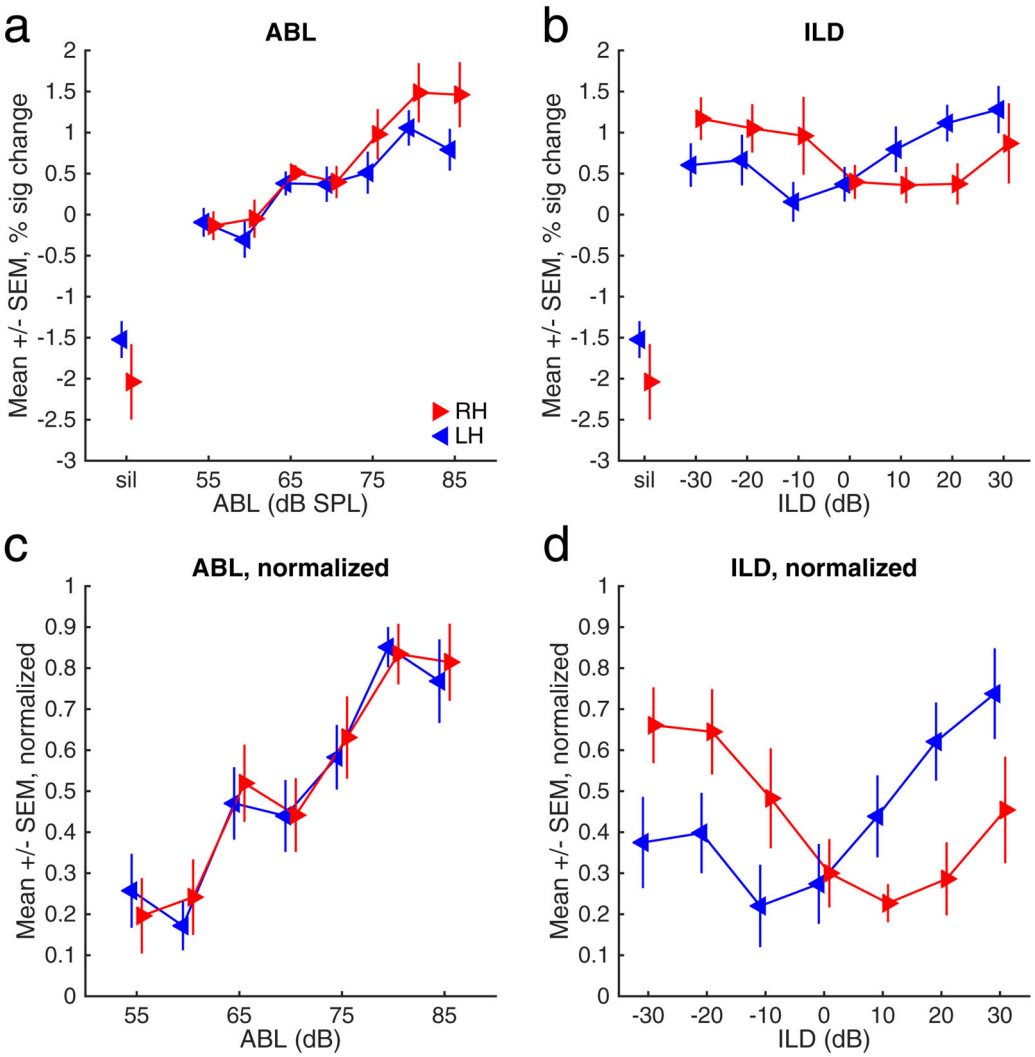

Fig. 4.

Response-ABL and response-ILD functions. Left-hemisphere data are plotted with blue leftward-pointing triangles; right-hemisphere data are plotted with red rightward-pointing triangles. Error bars indicate ±1 standard error of the mean across subjects. (a): Response-ABL functions for diotic stimuli (positive diagonal of Fig. 2), plotted in units of percent signal change relative to overall baseline. Overall sound response is evidenced by roughly 1.5–2% BOLD-magnitude reduction following silent blocks (“sil”). Across a 30 dB range of ABL, responses increased in a roughly monotonic fashion, by approximately 1.5% in both hemispheres. (b): Response-ILD functions (see negative diagonal of Fig. 2), also in units of percent signal change. In both hemispheres, responses varied significantly, but by approximately 1%, across a 60 dB range of ILD. Largest responses were observed for large contralateral values of ILD; in contrast, response minima were found for moderate (10–20 dB) ipsilateral ILD values. (c) and (d) plot response-ABL and response-ILD functions, respectively, computed after normalizing each subject’s function to the range [0 1] across ABL or ILD (silent blocks were omitted from this analysis). Normalization reveals a clearer correspondence of tuning functions across hemispheres.

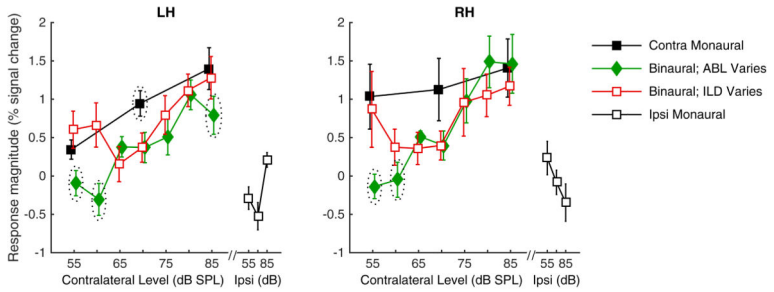

Fig. 5.

BOLD-response data for all tested binaural and monaural intensity combinations (Fig. 2), plotted as a function of intensity in the contralateral ear. Left and right panels plot data for left (LH) and right (RH) hemispheres, respectively. In each panel, four lines plot responses for specific stimulus combinations: **Black squares** plot responses to 55, 70, and 85 dB monaural stimulation of the contralateral ear (white text in Fig. 2). **Green diamonds** plot responses to binaural stimulation of both ears at equal intensity, with average binaural level (ABL) ranging 55–85 dB SPL (green text in Fig. 2), and **red open squares** plot responses for sounds varying in ILD (green text in Fig. 2); that is, ipsilateral intensity decreases from 85 to 55 dB as contralateral intensity increases from 55 to 85 dB and vice versa. On a separate axis indicating ipsilateral intensity, open (white) squares plot responses to ipsilateral monaural stimulation at 55, 70, and 85 dB SPL. Error bars indicate ±1 standard error of the mean across subjects in each case. Dotted ellipses indicate data points that differed significantly from all other conditions at that intensity (bootstrapped paired-differences test, $p < .05$). Note that data for the 70 dB SPL stimulus combinations which appear in Fig. 3 are also plotted here. As illustrated in the previous figure, left-hemisphere responses were significantly greater to contralateral than to binaural stimulation at that intensity; right-hemisphere responses exhibited a similar trend that was not statistically significant (note presence and absence of dotted ellipse for LH and RH data, respectively).

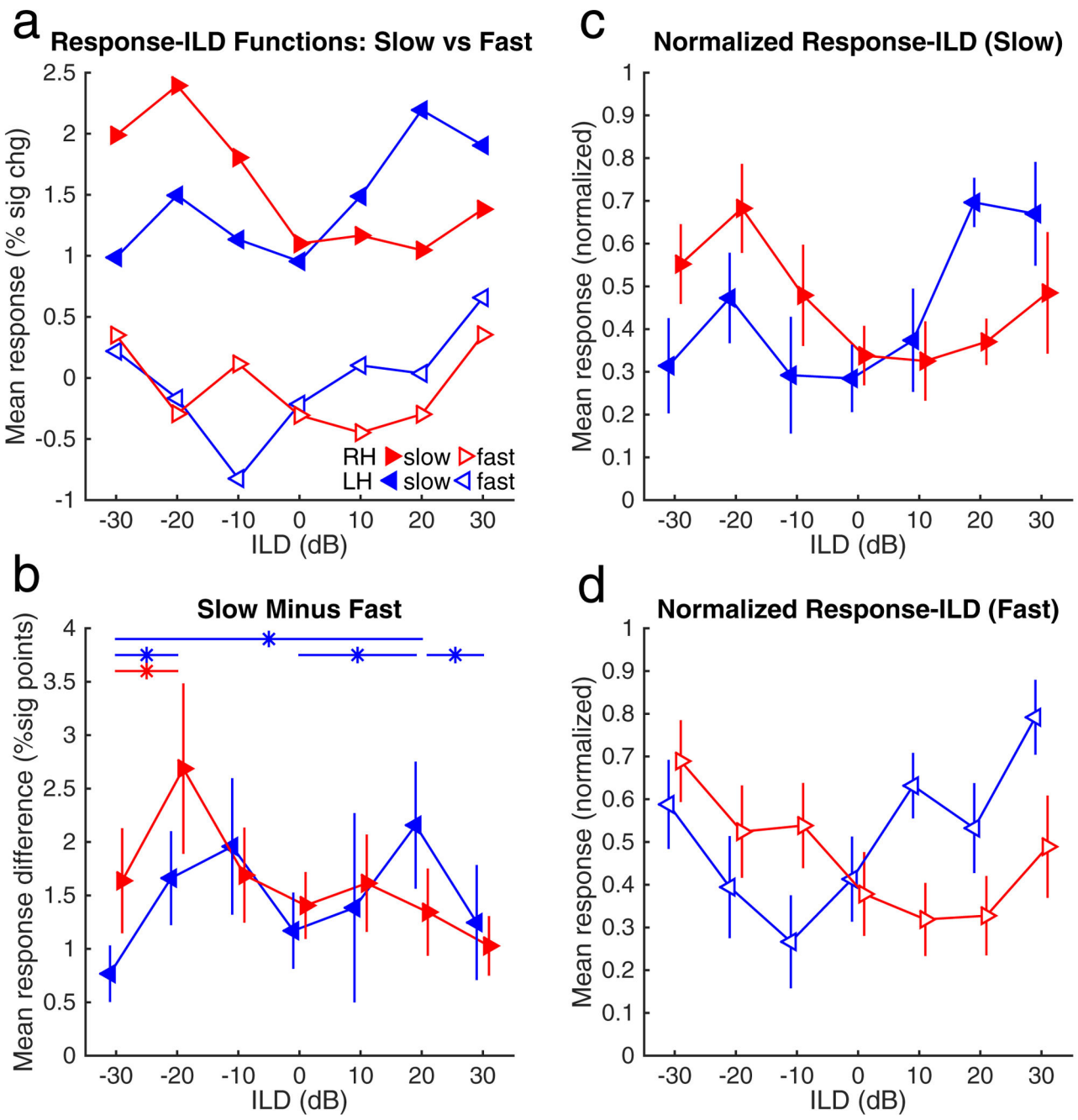

Fig. 6.

Effects of stimulus presentation rate. (a): Response-ILD functions, in units of percent signal change, are plotted separately for different conditions of stimulus presentation rate (filled symbols: “slow”, open symbols and dashed lines: “fast”). Although error bars are omitted for clarity, larger responses were observed for slow presentation rates, consistent with rate-dependent response adaptation (Harms and Melcher, 2002). The difference between these functions (b) was consistently positive, but modulated by ILD so that in some cases greater habituation effects were observed away from 0 dB ILD (e.g., 20 dB contralateral ILD).

Horizontal lines marked with asterisks at top indicate significant pairwise differences at FDR < .05. (c) and (d) plot normalized response-ILD functions for “slow” and “fast” presentations only. Comparison of the function shapes reveals an inward shift in tuning, which encompassed the midline (0 dB ILD) during “fast” presentations but was more selective for contralateral ILD values during “slow” presentations. Overall, response functions remained symmetrically similar across hemispheres, crossing over near 0 dB ILD, at both presentation rates.

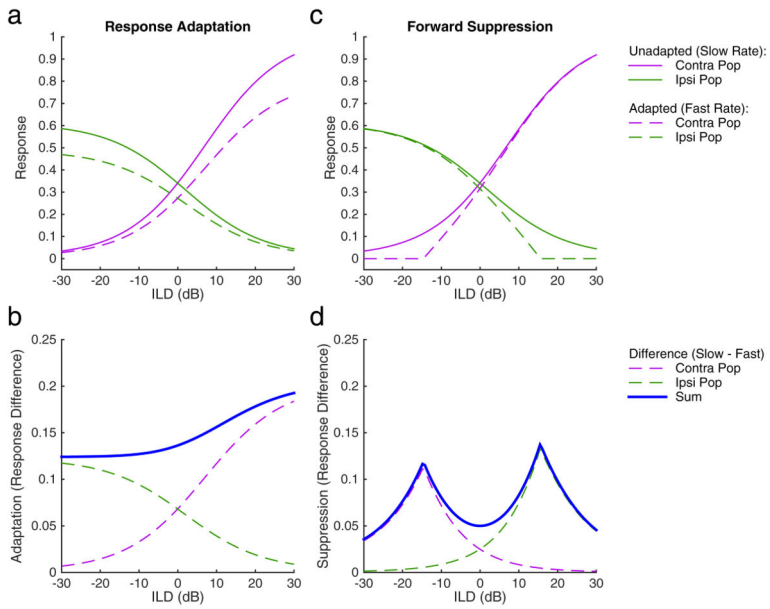

Fig. 7.

Descriptive models of rate-dependent adaptation (a–b) and forward suppression (c–d) in an opponent-channel framework. (a): Modeled response-ILD functions for contralateral (violet) and ipsilateral (green) populations within a single (left) AC hemisphere. Solid lines plot functions corresponding to relatively unadapted responses (i.e., to slow presentation rates); dashed lines plot functions corresponding to adapted responses (i.e., to fast presentation rates). Note the slight asymmetry in response magnitude across contralateral and ipsilateral populations to illustrate the greater weighting of contralateral than ipsilateral populations. In (a), response adaptation is proportional to the magnitude of response within each population. (b): Dashed lines plot the magnitude of response adaptation in each population, as a function of ILD. Thick solid line plots the sum for comparison to BOLD response differences in Fig. 6b. Purely response-dependent adaptation as implemented in (a) and (b) results in greater adaptation for sounds which drive greater overall response – corresponding in this case to contralateral (positive) ILD values that drive the relatively stronger contralateral population response. (c): Response-ILD functions as in (a), but with adapted responses (dashed lines) corresponding to forward suppression of each population's response by the opposing population. Response reduction is proportional to the ratio of activity in opponent channels, but constrained to avoid negative responses. (d): Response differences computed for the forward-suppression model, plotted as in (b). Note that the greatest suppression of responses is observed for intermediate ILD values that drive both the contralateral and ipsilateral populations, but in asymmetric fashion.